Theoretical Analysis of K Adsorption on TiO_2(110) Rutile Surface

C. J. Calzado,* M. A. San Miguel, and J. F. Sanz

Departamento de Química-Física, Facultad de Química, Universidad de Sevilla, E-41012, Sevilla, Spain

Received: July 13, 1998; In Final Form: November 9, 1998

The interaction between K atoms and the (110) rutile surface was analyzed by performing ab initio Hartree−Fock calculations and molecular dynamics simulations, demonstrating that the interaction is mainly electrostatic. The preferential sites of adsorption were determined, and the effect of the coverage was studied. Our results show a maximum coverage from which it is not possible to model the deposition process by a classical method. This limit corresponds to a K/Ti(surface) ratio of 0.40, which could be related to the maximum decrease of the work function found experimentally.

Introduction

For its simple structure and catalytic properties, TiO_2 (rutile) is one of the most studied solids in materials science.[1] This system is a nonmagnetic insulator, with a band gap of approximately 3 eV,[2] situated between the conduction band, which is essentially Ti 3d character, and the valence band of predominantly O 2p character.[3]

Among the low index faces, the (110) surface is the most stable.[4] The stoichiometric surface has no occupied gap states and is inert to chemisorption of a wide variety of molecules.[1] However, its catalytic activity can be promoted by means of oxygen vacancies or by adsorbing metal atoms.[1,5−11] Both of them induce occupied gap states placed around 1 eV below the conduction band edge.[5−22] Different spectroscopic evidences[5−23] have shown that these states are predominantly Ti 3d in character. These results reveal the presence of reduced Ti atoms in the system. They can be produced by means of charge-transfer processes from the adsorbed metal to the surface or because of the reorganization of electrons left upon removal of the oxygen atoms, in both cases leading to Ti^{3+} species.[1]

Aside from catalysis, another important application of the metal deposition on the surface is to diminish the work function. Given the low first ionization potential of the alkali metals (AM), they have been extensively used to promote this surface.[7,8,15−22] For the (110) surface, the adsorption of Na induces a lowering of the work function of 3.4 eV,[15,22] and around 2.0 eV in the K case.[17−19,22]

The geometric properties of AM deposited on TiO_2(110) have been the subject of controversy during the past few years, the sodium deposition having been the most often studied. Onishi et al.,[15] from the observed c(4 × 2) LEED pattern at 0.5 ML Na coverage, proposed a model consisting of Na bound to two protruded surface oxygen atoms and one basal oxygen atom in a symmetric arrangement. Later, Murray et al.,[21] based on STM experiments on a reduced TiO_2(110)−(1 × 2) surface, suggested another model where Na atoms conserve the tri-coordination, binding one bridging oxygen and two basal oxygen atoms. Recently, Nerlov et al.[20] have shown that both arrangements correspond effectively to a different structure of the surfaces.

In a previous work,[24] we performed ab initio embedded cluster calculations on the Na/TiO_2(110)−(1 × 1) and determined the selectivity of the reduction. Furthermore, the geometry optimization of the adsorbed Na upon charge transfer leads to a structure consistent with the Nerlov model.[20] By means of MD simulations of surfaces with a dense coverage,[25] we found a predominant alternated arrangement around the protruded oxygen rows, in which Na atoms mostly present the tri-coordination proposed by Nerlov et al.[20]

As for the K adsorption process, the number of related experimental studies[16−19,22] have been relatively scarce when compared to those mentioned above. In this case and up to date, no LEED pattern of the K/TiO_2(110) has been observed. According to the Heise and Courths results,[17,18] there exists a critical coverage at which the work function shows the maximum decrease. Coverage of 1 ML was established by the appearance or disappearance of the potassium plasmons, and then, the precise number of K atoms corresponding to this coverage was unknown.[17,18] In this context, the critical coverage was found at 0.37 ML. Throughout this study, we will refer to coverage (R) defined as the ratio between the number of adsorbed K atoms and surface Ti atoms (both 5- and 6-fold Ti atoms), in such a way that $R = 1$ corresponds to a K surface density of 1.0404×10^{15} K atoms/cm^2.

In this work, the geometric and electronic features of the K deposition on TiO_2(110) surface were approached by means of a theoretical scheme by combining ab initio HF calculations and classical molecular dynamics simulations in the same way as the Na case was carried out.[24,25] Since the processes are similar, it seems reasonable to assume the techniques used are reliable. Therefore, the importance of the results lies in their predictive character as a complement of the few experimental findings about the behavior of the K atoms on the TiO_2(110) surface.

Ab Initio Calculations

Both the nature of the K/TiO_2 interaction and the selectivity of the reduction process were analyzed by means of ab initio HF embedded cluster calculations. As is well-known, this method is adequate to study localized phenomena. The active site is explicitly treated, and the environment is modeled by an array of point charges representing the effect of infinite crystal potential. The cluster model employed in this work was

* Author to whom correspondence should be addressed. E-mail: calzado@cica.es.

10.1021/jp982994+ CCC: $18.00
Published on Web 01/05/1999

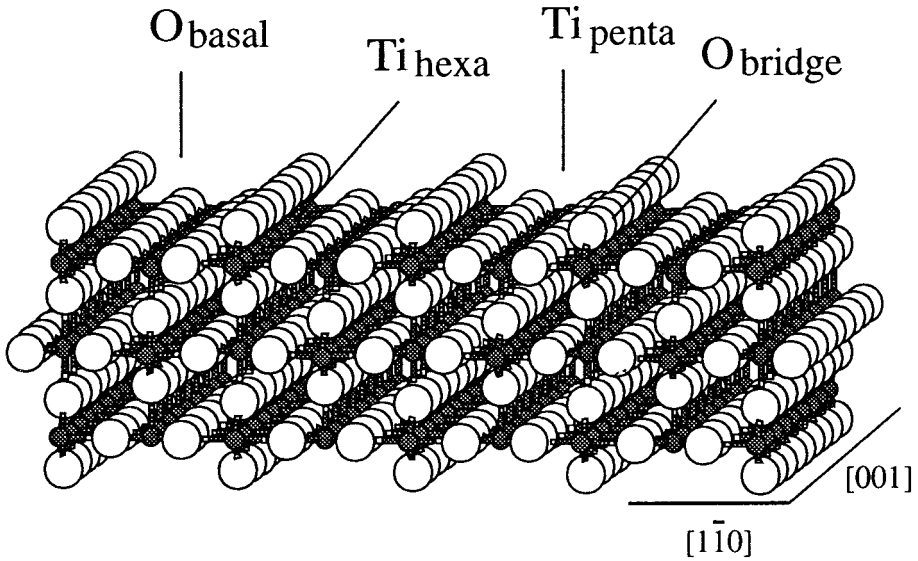

Figure 1. A general view of the relaxed (110)−(1 × 1) rutile surface from molecular dynamics simulations.

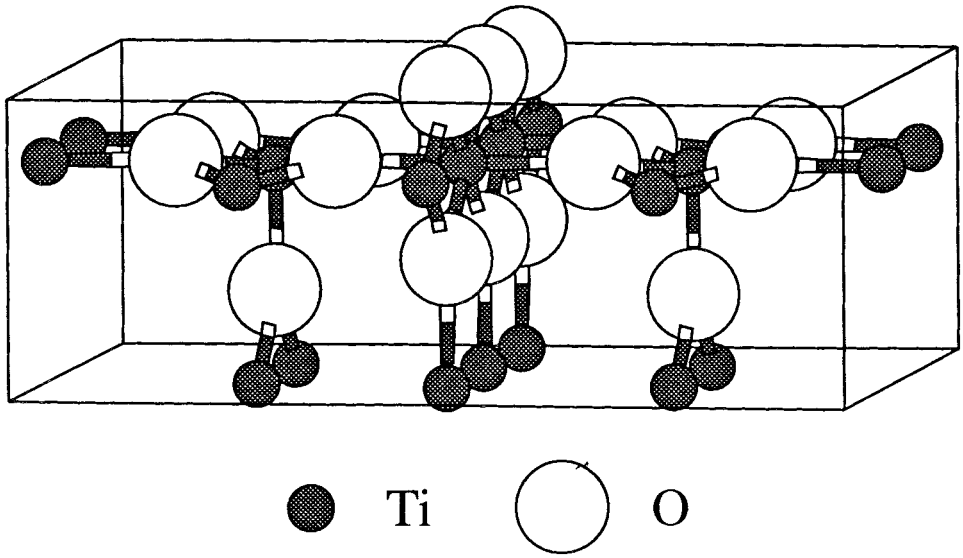

Figure 2. The cluster model Ti_4O_{16}. Dark and white balls indicate Ti and O atoms, respectively.

discussed previously,[24,25] and only a brief description will be outlined here.

Figure 1 shows a view of the (110) rutile surface. Five- and 6-fold coordinated Ti atoms can be distinguished. An adequate model to represent both of them could be a cluster of formula Ti_4O_{16}, where two pairs of penta- and hexa-coordinated Ti atoms are included (Figure 2). This cluster was surrounded by an array of 1404 formal point charges. In the cluster-point charges interface, a set of 17 Ti total ion potentials (TIP) is added to avoid an excessive polarization of boundary oxygen ions.

The core electrons of the cluster atoms were described by using the effective core potentials (ECP). For titanium and potassium atoms (10 and 18 core electrons, respectively), the ECPs proposed by Hay and Wadt were used,[26] and the ECPs of Stevens et al.[27] for the 1s electrons of the oxygen atoms were selected. The basis sets for the valence electrons were (10s5p5d)/[2s2p2d] for Ti, (3s1p)/[2s1p] for K,[26] and (4s4p)/[2s2p] for O atoms.[27] For the Ti-TIP representation, the large core effective potential of Hay and Wadt was chosen.[26]

It is well-established experimentally and theoretically that when the K atom approaches the surface, it transfers the 4s electron to the surface and becomes a K^+ ion.[17−19,22,24,25,28] Two different Ti atoms can be reduced, and as has been mentioned above, both of them are included in our cluster. Unrestricted-spin Hartree−Fock calculations of K/Ti_4O_{16} system show that only a 5-fold Ti atom is reduced. This process is associated with the occupation of a molecular orbital, essentially the Ti dx^2-y^2, placed between occupied 2p oxygen-like molecular orbitals (valence band) and virtual 3d titanium-like molecular orbitals (conduction band). This result is in good agreement with the emission found at about 1 eV below the bottom of the bulk conduction band in UPS spectra.[17−19]

The UHF geometry optimization leads to a stationary point in which the alkali metal binds to two protruded oxygen atoms, and to a basal one at a longer distance. This tri-coordination minimizes the repulsions between the K and its Ti neighbors, and maximizes the attractive interactions (Figure 3). This equilibrium geometry is similar to the model proposed in the Na/TiO_2(110)−(1 × 1) system from photoemission measurements by Nerlov et al.[20] In such a case, the Na/TiO_2 adsorption model coincides adequately with our previously reported simulations.[25] However, for the K/TiO_2 interaction, there is not an experimental adsorption pattern, and hereby the importance of this theoretical prediction.

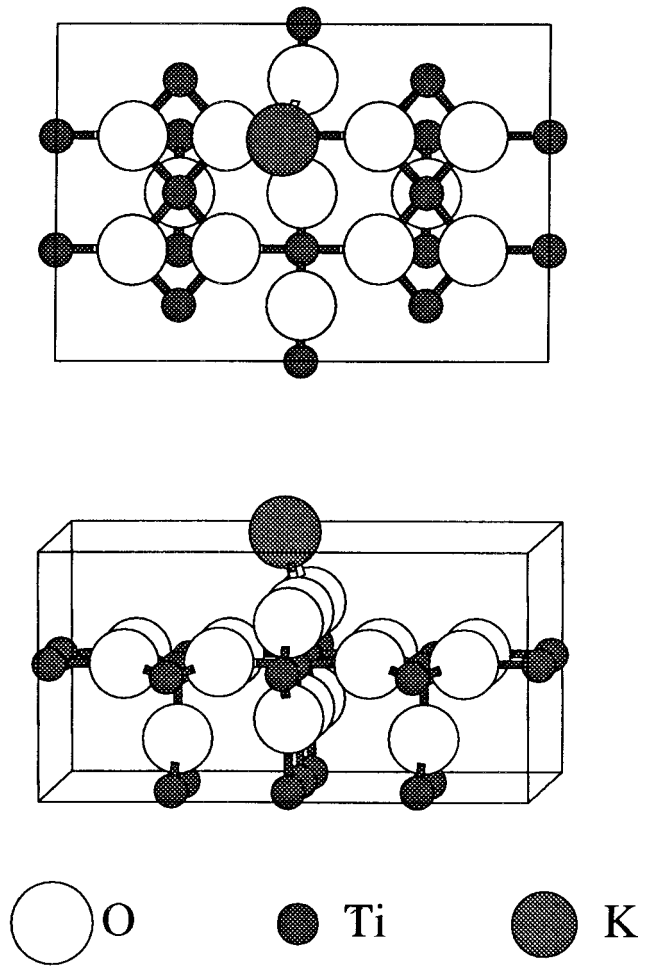

Figure 3. The optimized adsorption geometry of K on the cluster. Top: view perpendicular to the (110) plane.

TABLE 1: Structural Parameters for the Alkali Metal (AM) Adsorption on the TiO_2(110) Surface Obtained from ab Initio UHF Calculations[a]

	Na	K
Ti_p	4.54	4.61
Ti_h	3.05	3.25
O_{bridge}	2.36	2.52
O_{basal}	3.38	3.51

[a] Units in angstroms.

The structural parameters for K and Na deposition are compared in Table 1. It can be seen that, in general, the K-surface distances are 0.2 Å longer than those corresponding to the Na case, which is consistent with the increase of the ionic radii.

To assess the character of the interaction, an *yz*-plane projection of the electrostatic potential on the (110) surface has been plotted in Figure 4. It corresponds to the plane containing the two 5-fold coordinated Ti atoms and the central bridge oxygen atom in the cluster. Solid and dashed lines indicate the positive and negative electrostatic potential, respectively. Since alkali atoms are positively charged species, the interactions with the surface will be attractive in the positions where the potential is negative, and as can be seen from Figure 4, these lines are close to the oxygen row. This fact indicates that the nature of the interaction alkali−surface after the reduction is essentially electrostatic, which explains the structural differences observed between the Na and K deposition processes.

Molecular Dynamics Simulations

We focus our interest on the dependence of structure and stability of the system as K coverage is increasing. Since we have demonstrated that the interactions between the particles in this system are mainly Coulombic type, a classical molecular dynamics approach will be used, as before.[24,25]

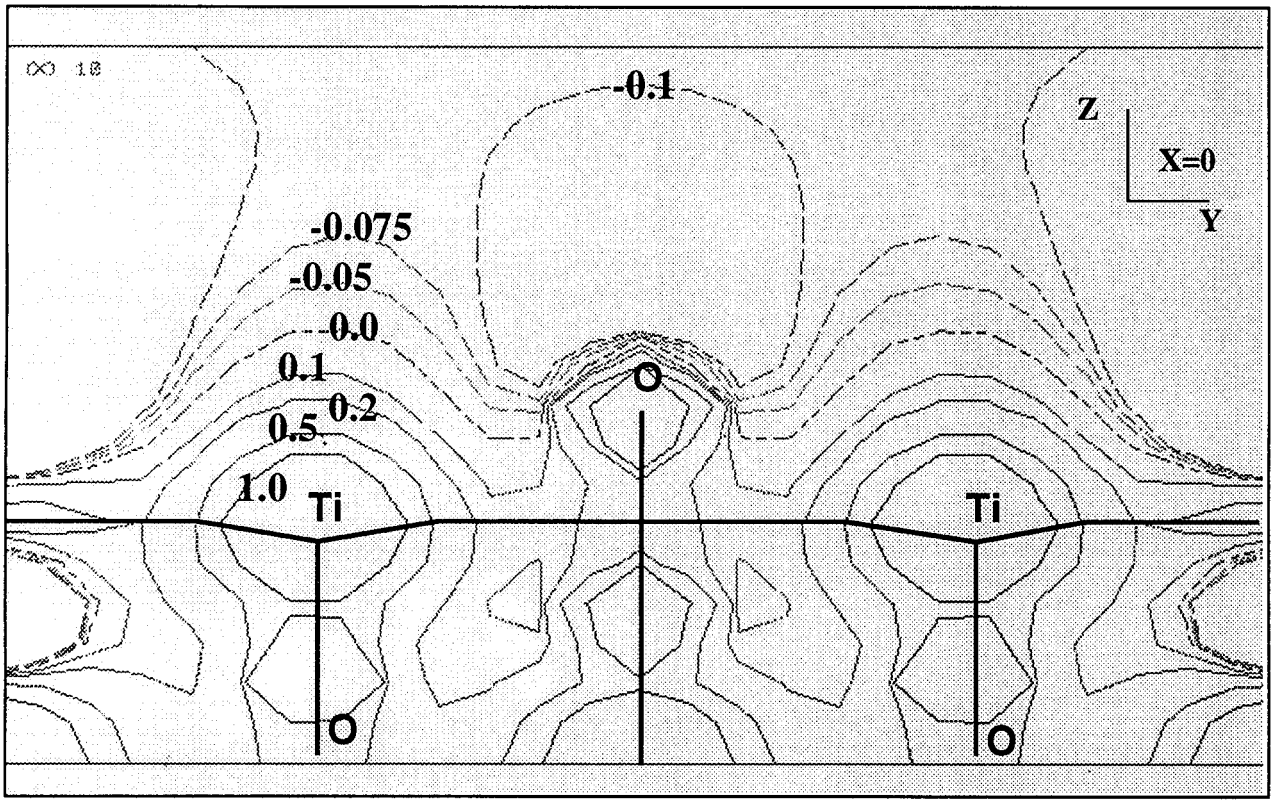

Figure 4. Electrostatic potential curves along *yz* plane for $x = 0$. The potential values are expressed in atomic units.

TABLE 2: Summary of the Pauling Pair Potential Parameters Used in the MD Simulations

	q (e)	σ (Å)
Ti(III)	1.196	0.68
Ti(IV)	2.196	0.68
O	−1.098	1.40
K	1	1.33

The (110) rutile surface was simulated by employing a computational box of 1620 particles (540 Ti + 1080 O). The interaction between particles was described by potential functions consisting of Coulombic and short-range terms:

$$V_{ij} = \frac{q_i q_j}{r_{ij}} + V_{ij}(s - r)$$

where q_i and q_j are the effective charges and r_{ij} the interparticle distance.

For the interaction between Ti and O atoms, a Buckingham-type short-range potential was used:

$$V_{ij}(s - r) = -\frac{C_i C_j}{r_{ij}^6} + f(B_i B_j) \exp\left(\frac{A_i + A_j - r_{ij}}{B_i + B_j}\right)$$

where the parameters A, B, C, and f were those given by Matsui et al.[29] For the interaction between K^+ and surface Ti and O atoms, a Pauling-type potential was chosen:

$$V_{ij}(s - r) = \frac{1}{\sigma_i + \sigma_j}\left(\frac{\sigma_i + \sigma_j}{r_{ij}}\right)^n$$

where σ_i and σ_j are the ionic radii for species i and j,[30] and parameter n was set to 9, according to Adams and McDonald.[31] The whole set of charges and ionic radii for this potential are summarized in Table 2.

As in the Na case, and according to the HF results, we have assumed that upon reduction, the new species on the surface are K^+ cations (q = 1e) and there are the same number of reduced pentacoordinated Ti atoms with an effective charge of +1.196 e, instead of the original charge of +2.196 e.

The K atoms were added to the surface until values for R reach 0.25, 0.30, 0.35, and 0.40. In every case the addition was performed on both sides of the slab to cancel out the dipole moment perpendicular to the surface.

Molecular dynamics simulations were performed in the microcanonical ensemble employing the SIMULA code.[32] Numerical integration of classical equations of motion was achieved by using the leapfrog algorithm with a time step of 1 fs. The temperature of the system was 300 K. All the simulations consisted of a initial stage of 3 ps in which the velocities of the particles were scaled at each time step in order to thermally equilibrate the system. After this period, another run of 8 ps was performed to ensure that the system is stabilized at 300 K. Finally, a production run of 5 ps was undertaken to calculate the statistics of the system.

TABLE 3: Structural Parameters for the Adsorption of One K Atom on the TiO_2(110) Surface Obtained from MD Simulations[a]

	model A	model B
K−Ti_p	4.5	5.0
K−Ti_h	3.5	3.5
K−O_{bridge}	2.8	2.7
K−O_{basal}	3.3	3.9

[a] Units in angstroms.

Some preliminary trial simulations at low coverage (where the K−K repulsions were negligible) were carried out to compare the structural parameters extracted from them with the corresponding ones to the UHF optimizations. Two main situations can be isolated from the final configurations of these simulations. They are depicted in Scheme 1. Site A consists of a tri-coordinated K atom binding two protruded oxygen atoms and a basal one, as was reported in the Na/TiO_2 deposition.[15,20,24,25] Site B corresponds to a K atom placed in the vertical position with respect to the 6-fold Ti atom and connected to only two bridge oxygen atoms. The most significant distances are collected in Table 3. UHF calculations show that site A is the most stable, while site B is a transition state between two A-type configurations. However, in the MD simulations at 300 K, an adsorbed alkali atom oscillates between both situations. This result would indicate that thermal fluctuations permit the system to overcome the activation barrier easily. Since UHF calculations are not dependent on the temperature, the resultant geometry can be seen as an intermediate situation between models A and B extracted from MD simulations. This is reflected from the distances reported in Table 3.

Figure 5 shows snapshots for initial and final configurations corresponding to the four coverages as set out above. To avoid the bias effect on the initial configurations, we selected a few models for each coverage: however, the results were not dependent on the original choices. In Figure 5, we reported only the most uniform initial distributions.

At lowest coverage, all the K atoms occupy sites A or B, although the preferential one is the former. For R = 0.30 (3.1212 × 10^{14} K atoms/cm^2), the situation is similar but the percentage of K atoms placed in site B increases. When the coverage reaches a value of 0.35 (3.6414 × 10^{14} K atoms/cm^2), some less stable situations, as model C indicated in Scheme 1, become significant. However, when the coverage is 0.40 (4.1616 × 10^{14} K atoms/cm^2) the configuration is not stable and it is not possible to place all the K atoms on the surface. It can be seen from the snapshot (lower panels) that the number of K atoms present in the final configuration is less than that in the initial structure.

SCHEME 1

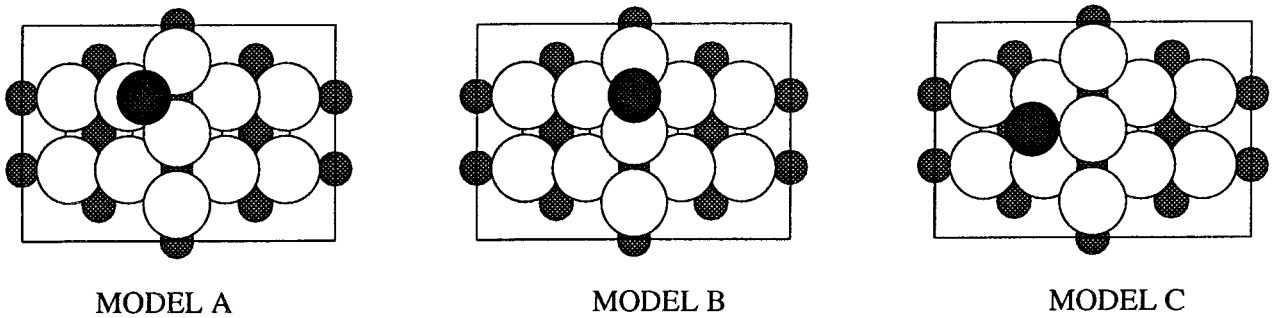

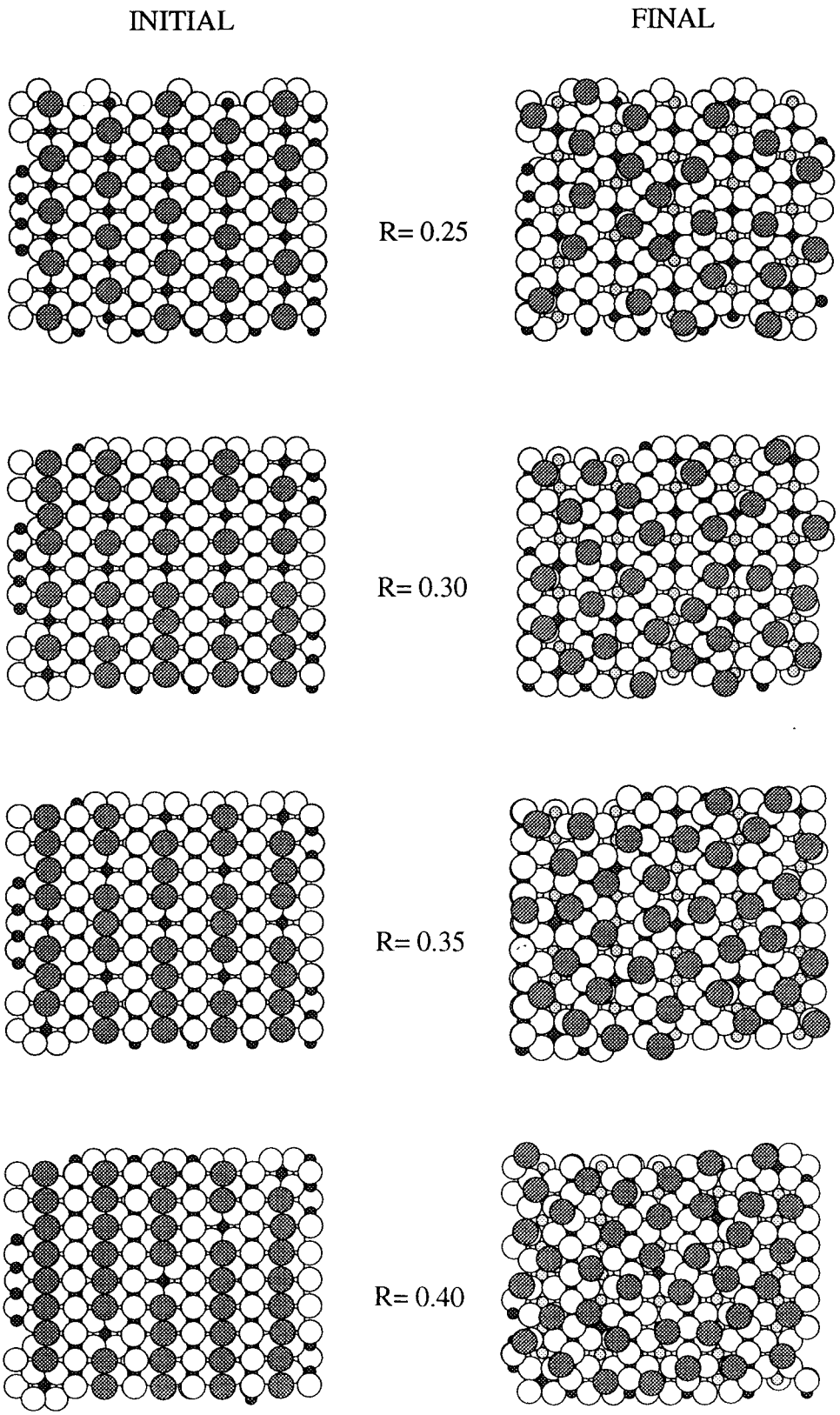

Figure 5. Snapshots for four coverages of K atoms on the TiO_2(110) surface. Left and right panels for initial and final configurations, respectively.

Therefore, our simulations indicate the presence of a maximum limit density for *R* between 0.35 and 0.4. In fact, it has been observed experimentally that the work function decreases linearly as the coverage increases up to a critical value (namely, 0.37 ML[17,18] or 0.5 ML,[22] depending on the calibration of the coverage scale in the experimental method). Increase of the work function at higher coverages than this limit indicates the presence of covalent interactions such as K−O bond formation and K−K clustering on the surface.[17−19,22]

An appealing point observed from our results is the appearance of a collective phenomenon similar to that found in our previous works on Na deposition.[24,25] On increasing the coverage, the alkaline atoms deepen in the surface. This effect means that the successive addition of alkali on the surface favors the

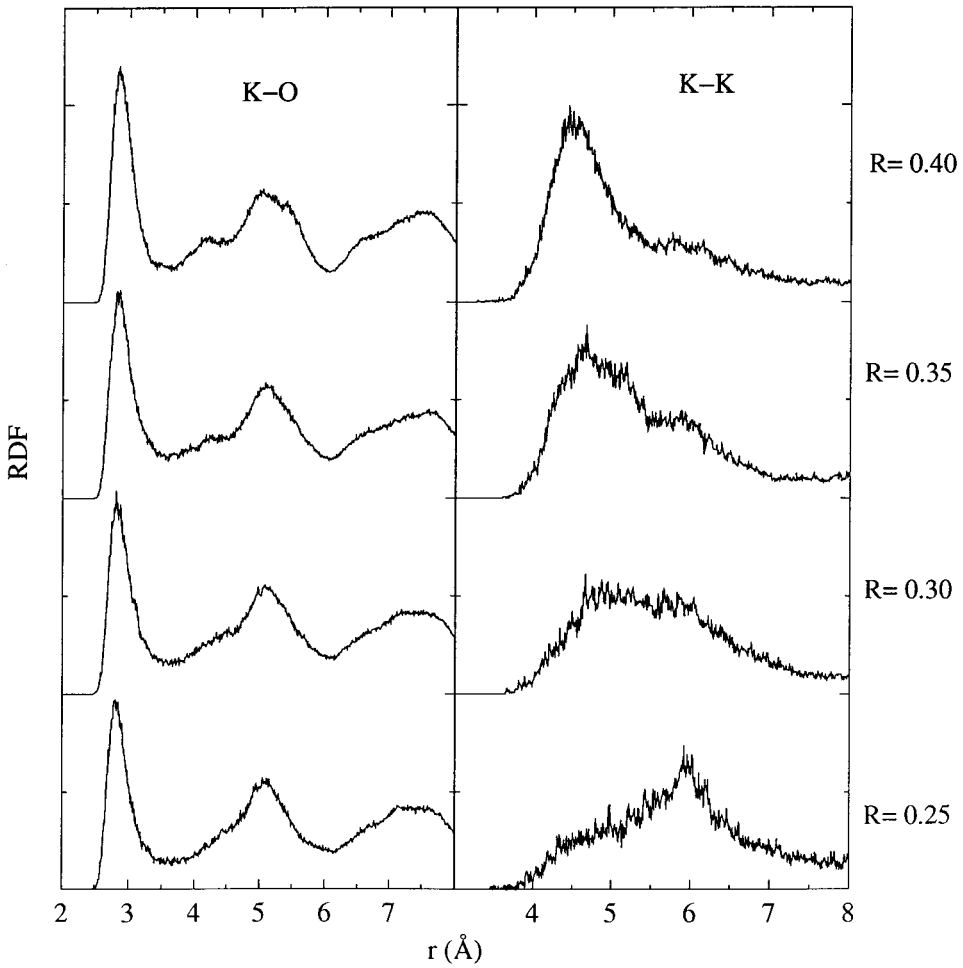

Figure 6. Radial distribution functions for K−O and K−K pairs at different coverages.

adsorption process up to critical coverage. It could be due to the decrease of the repulsion forces between adsorbed K atoms and surface Ti atoms as the number of reduced Ti atoms increases.

Some interesting structural aspects can be analyzed from the radial distribution functions (RDF). Figure 6 shows these curves for K−K and K−O pairs. In respect to the former, it can be seen that as the coverage increases the K−K broad band centered roughly at 6.0 Å transforms to a well-defined peak situated at 4.5 Å at the highest coverage. This fact would indicate the appearance of an ordering process when the coverage reaches the critical value. The absence of order for $R < 0.4$ is consistent with the observance of a no reconstructed LEED pattern at room temperature.[19] The K atoms at the critical coverage exhibit the most uniform distribution, at which every K−K distance is equal to 4.5 Å and the main factors controlling the allocation of the atoms are the alkali−alkali Coulombic repulsive forces. It can be seen from a careful analysis that this structure is close to a bi-dimensional hexagonal compact package as the (111) metal plane.

As for the K−O pairs, two well-defined peaks around 3 and 5 Å can be distinguished. They are associated with $K-O_{bridge}$ and $K-O_{basal}$ distances, respectively. The presence of a small shoulder close to the second peak can also be observed, which could be assigned to the distances between K atoms and the nearest basal oxygen atoms. This peak is more defined at high coverages due, presumably, to the decrease of mobility on the surface.

To analyze the diffusion processes related to the adsorbed species, the van Hove autocorrelation function has been calculated. It gives the probability of finding an atom displaced from its original position after a time *t*. Figure 7 shows these functions at 1 ps for different coverages. The most significant mobility is found at $R = 0.25$, where the atoms diffuse by hopping to far distances. When the coverage reaches maximum value, the function exhibits a curve with a main sharp peak at 0.5 Å corresponding to the thermal vibrations and a short and little tail indicating that the number of jumping atoms is certainly scarce.

Conclusions

In this work, we performed HF calculations and MD simulations to study the K deposition on TiO_2(110) rutile surface. From the former we have demonstrated that the reduction is selective and it is associated with a charge transfer from the alkali to the 5-fold surface titanium atoms. Upon this redox process, the electrostatic forces control the interactions between the alkali atom and the surface. The most favorable adsorption geometry determined by HF calculations and from MD simulations is the same and consists of a K atom binding two protruded oxygen atoms and a basal one.

Three main conclusions can be extracted from our simulations. The first is the variation of K arrangements as a function of the coverage. A preferential tri-coordinated K model is observed at low coverages. When the number of K atoms on the surface increases, the most stabilized situation corresponds to a K atom bound to two bridge oxygen atoms, practically in the vertical of the 6-fold Ti atom. When the coverage reaches the critical value, ordering is governed by the repulsive K−K

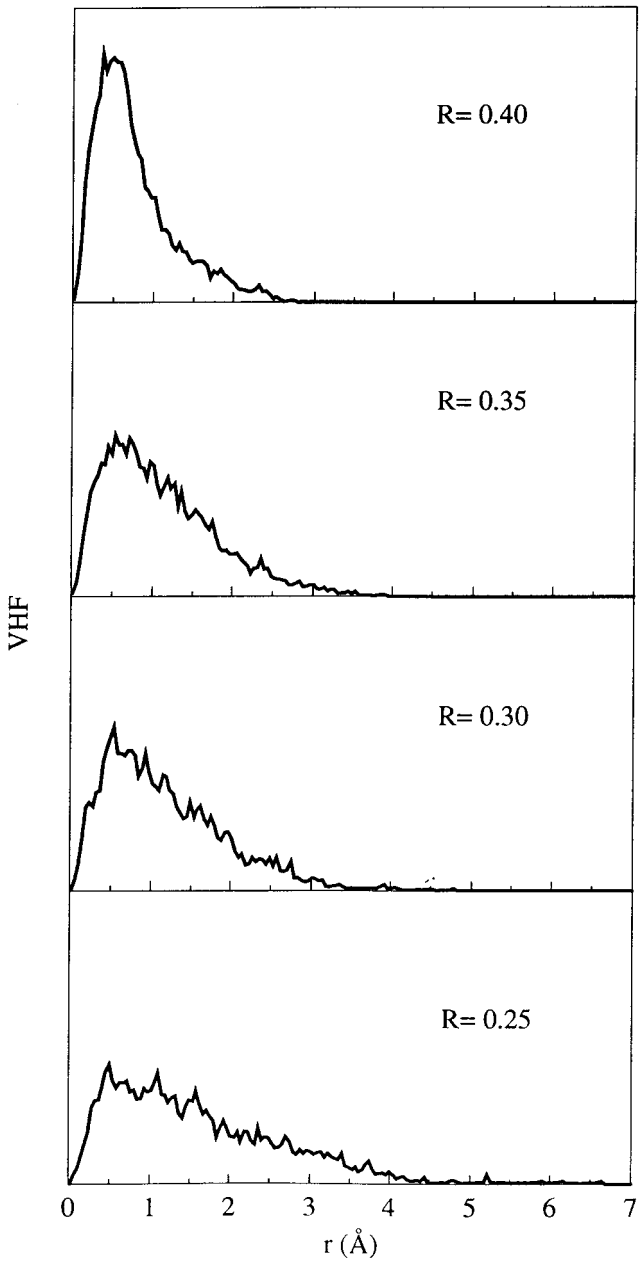

Figure 7. Van Hove autocorrelation functions for K species obtained from MD simulations at 1 ps.

interactions, leading to a hexagonal compact pattern. The second conclusion is the validity of the classical simulations when the adsorption process is controlled by electrostatic interactions. The last one is the prediction of the critical coverage of approximately $3.64-4.16 \times 10^{14}$ K atoms/cm^2, which could be associated with the maximum decrease of work function experimentally observed.

On the other hand, since $R = 0.40$ corresponds to the limit of our model, the adsorbed K ordering found could be an artifact and could not respond to a real situation. Anyway, the simulations indicate the appearance of new chemical processes in which the electrostatic forces are less important. In fact, the formation of KO_x species beyond the maximum coverage has been experimentally reported, implying the participation of covalent contributions demanding more sophisticated approaches to model them.

Acknowledgment. This work was supported by the DGICYT (Spain, Project No. PB95-1247). C.J.C. and M.A.S.M. are grateful to Dr. J. J. Calvente for fruitful discussions and helpful suggestions.

References and Notes

(1) Henrich, V. E.; Cox, P. A. *The Surface Science of Metal Oxides*; Cambridge University Press: Cambridge, 1994.
(2) Strehlow, W. H.; Cook, E. C. *J. Phys. Chem. Ref. Data* **1973**, *2*, 163.
(3) Cox, P. A. *Transition Metal Oxides*; Clarendon Press: Oxford, 1995.
(4) Cox, P. A.; Dean, F. W. H.; Williams, A. A. *Vacuum* **1983**, *33*, 839.
(5) Linsebigler, A. L.; Lu, G.; Yates, J. T. *Chem. Rev.* **1995**, *95*, 735.
(6) Barteau, M. A. *Chem. Rev.* **1996**, *96*, 1413.
(7) Onishi, H.; Aruga, T.; Egawa, C.; Iwasawa, Y. *J. Chem. Soc., Faraday Trans. 1* **1989**, *85*, 2597.
(8) Onishi, H.; Iwasawa, Y. *Catal. Lett.* **1996**, *38*, 89.
(9) Prabhakaran, K.; Purdie, D.; Casanova, R.; Muryn, C. A.; Hardman, P. J. *Phys. Rev. B* **1992**, *45*, 6969.
(10) See, A. K.; Bartynski, R. A. *Phys. Rev. B* **1994**, *50*, 12064.
(11) Okamura, T.; Okushi, H. *Jpn. J. Appl. Phys.* **1993**, *32*, L454.
(12) Egdell, R. G.; Eriksen, S.; Flavell, W. R. *Solid State Commun.* **1986**, *60*, 835.
(13) Aiura, Y.; Nishihara, Y.; Haruyama, Y.; Komeda, T.; Kodaira, S.; Sakisaka, Y.; Maruyame, T.; Kato, H. *Physica B* **1994**, *194*−*196*, 1215.
(14) Mohamed, M. H.; Sadeghi, H. R.; Henrich, V. E. *Phys. Rev. B* **1988**, *37*, 8417.
(15) Onishi, H.; Aruga, T.; Egawa, C.; Iwasawa, Y. *Surf. Sci.* **1988**, *199*, 54.
(16) Casanova, R.; Prabhakaran, K.; Thornton, G. *J. Phys. Condens. Matter.* **1991**, *3*, 591.
(17) Heise, R.; Courths, R. *Surf. Sci.* **1995**, *331*−*333*, 1460.
(18) Heise, R.; Courths, R. *Surf. Rev. Lett.* **1995**, *2*, 147.
(19) Lad, R. J.; Dake, L. S. *Mater. Res. Soc. Symp. Proc.* **1992**, *238*, 823.
(20) Nerlov, J.; Christensen, S. V.; Weichel, S.; Pedersen, E. H.; Moller, P. J. *Surf. Sci.* **1997**, *371*, 321.
(21) Murray, P. W.; Condon, N. G.; Thornton, G. *Surf. Sci.* **1995**, *323*, L281.
(22) Souda, R.; Hayami, W.; Aizawa, T.; Ishizawa, Y. *Surf. Sci.* **1993**, *285*, 265.
(23) Zhang, Z.; Jeng, S. P.; Henrich, V. E. *Phys. Rev. B* **1991**, *43*, 12004.
(24) San Miguel, M. A.; Calzado, C. J.; Sanz, J. F. *Int. J. Quantum Chem.* **1998**, *70*, 351.
(25) San Miguel, M. A.; Calzado, C. J.; Sanz, J. F. *Surf. Sci.* **1998**, *409*, 92.
(26) Hay, P. J.; Wadt, W. R. *J. Chem. Phys.* **1985**, *82*, 270; **1985**, *82*, 284; **1985**, *82*, 299.
(27) Stevens, W. J.; Basch, H.; Krauss, M. *J. Chem. Phys.* **1984**, *81*, 6026.
(28) Lindan, P. J.; Muscat, J.; Bates, S.; Harrison, N. M.; Gillan, M. *Faraday Discuss.* **1997**, *106*, 135.
(29) Matsui, M.; Akaogi, M. *Mol. Simul.* **1991**, *6*, 239.
(30) Pauling, L. *The Nature of the Chemical Bond*, 3rd ed.; Cornell University Press: Ithaca. New York, 1960; p 514.
(31) Adams, D. J.; McDonald, I. R. *Physica B* **1970**, *79*, 159.
(32) San Miguel, M. A. Ph.D. Thesis, University of Sevilla, Sevilla, Spain, 1998.